

Pyrrole-based metallo-macrocycles and cryptands

Paul D. Beer,^{*a} Andrew G. Cheetham,^a Michael G. B. Drew,^b O. Danny Fox,^a Elizabeth J. Hayes^a and Toby D. Rolls^a^a Department of Chemistry, Inorganic Chemistry Laboratory, University of Oxford, South Parks Road, Oxford, UK OX1 3QR. E-mail: paul.beer@chem.ox.ac.uk^b Department of Chemistry, University of Reading, Whiteknights, Reading, UK RG6 6AD

Received 15th October 2002, Accepted 9th December 2002

First published as an Advance Article on the web 21st January 2003

The synthesis of dithiocarbamate ligands based on a pyrrole framework is reported. These ligands self-assemble with zinc(II), nickel(II) and copper(II) to afford neutral, dinuclear metallomacrocycles and trinuclear metallocryptands. The assembled metallo compounds have been characterised by a range of techniques, including ¹H NMR, UV-vis spectroscopy, elemental analysis, mass spectrometry and X-ray crystallography. Some preliminary anion binding studies have also been conducted, using electronic spectroscopy and electrochemistry. The nickel macrocycles showed some affinity for acetate, whereas the copper cryptand showed affinity for benzoate anions. The copper cryptand also exhibited a significant electrochemical response to a range of anions.

Introduction

The synthesis of two- and three-dimensional macrocyclic and cage-like host molecules using metal-directed self-assembly is a current area of intense research activity.^{1–8} Through prudent choice of multidentate ligand and stereochemical requirement of the mediating metal ion, the resulting self-assembled poly-metallic structures may be designed to exhibit unique redox, magnetic and photochemical properties, and have the potential to bind, sense and react together with guest substrates.^{9–12} Because assembly of such receptors with labile metal ions is often a thermodynamically driven process, yields of self-assembled products can often far exceed those created by formation of covalent bonds.

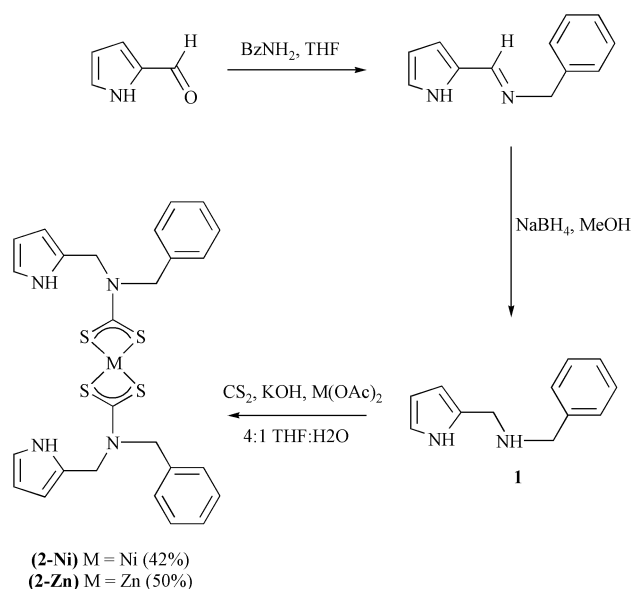
Presently the field is dominated by square planar platinum(II) and palladium(II) metals in combination with various oligopyridine ligands,^{2,13,14} copper(I), nickel(II), silver(I), and iron(II) helical structures of oligobipyridyls^{12,15} and pseudo-octahedral titanium(IV), aluminium(III), iron(III) and gallium(III) complexes of oligocatecholate ligands leading to triple helicates and tetrahedral clusters.^{15,16}

To date the use of pyrrole-based ligands in metal-directed self-assembly has born great similarity to that of pyridyl-based ligands in the field, with the pyrrole N atom coordinating directly to a metal ion.^{17–20} Sessler and coworkers have used calixpyrroles for anion recognition,^{21,22} and the tripodal pyrrole synthon has already been used to synthesise cryptands which have been shown to bind small neutral molecules.²³ We report here the metal-directed self-assembly of novel pyrrole-based metallo-macrocycles and cryptands which are designed to coordinate anions *via* their pyrrole NH groups, precluding direct metal ion coordination to the deprotonated pyrrole N atoms. This has necessitated the incorporation of another ligand into the target structures, namely the dithiocarbamate (dtc) group, which we have recently used as a self-assembling construction motif in the synthesis of nanosized resorcarene-based transition metal polymetallic assemblies,^{24,25} copper(II)-dtc macrocycles^{26–28} and catenanes.²⁹

Results and discussion

Synthesis of acyclic and macrocyclic pyrrole metal dtc complexes

Acyclic “model” pyrrole–metal–dtc complexes were initially prepared *via* the synthetic procedure shown in Scheme 1. The nickel(II) and zinc(II) dtc complexes of **2** were prepared in a one-pot synthesis from amine **1** by reaction with carbon disulfide, KOH and either nickel(II) or zinc(II) acetate in a 4 : 1 THF–H₂O



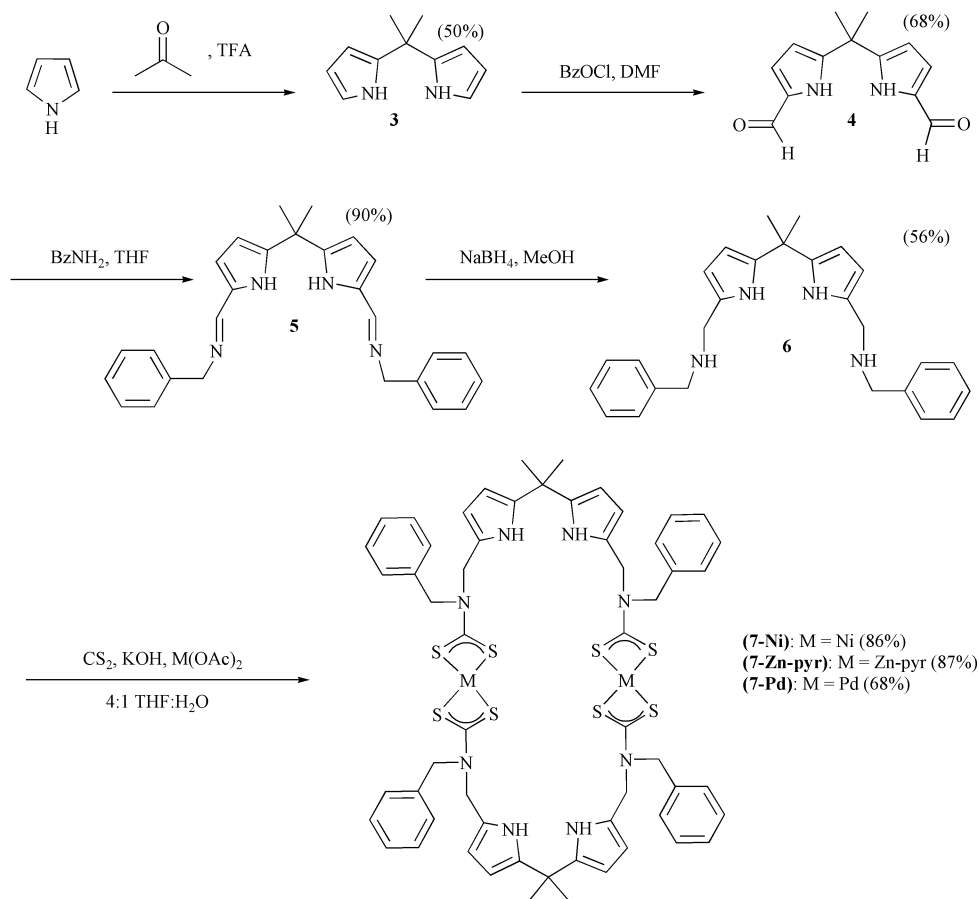
Scheme 1 Preparation of acyclic transition metal complexes of pyrrole-based ligands.

solvent mixture. Recrystallisation from dichloromethane–ethanol mixtures afforded analytically pure complexes in yields of 42% for (**2-Ni**) and 50% for (**2-Zn**).

The pyrrole-based metallo-macrocycles were synthesised according to the procedure illustrated in Scheme 2. Vilsmeier–Haack formylation of dimethyldipyrromethane **3** gave **4** which was condensed with two equivalents of benzylamine to give the Schiff base compound **5** in 89% yield. Sodium borohydride reduction in methanol afforded the diamine **6** as a white solid in 56% yield. The metallo-macrocycles (**7-M**, M = Ni, Zn-pyr, Pd) were prepared in very good yields by the same one-pot procedure with carbon disulfide, base and either nickel(II) acetate, K₂PdCl₄ or zinc acetate in 4 : 1 THF–H₂O solutions. The binuclear zinc(II) metallo-macrocycle was isolated as the pyridine adduct.

Characterisation

All these new acyclic and macrocyclic metal–dtc complexes were characterised by a variety of techniques including ¹H NMR spectroscopy, UV-vis spectroscopy, mass spectrometry, elemental analysis (see Experimental section) and in some cases by X-ray crystal structure determination.



Scheme 2 Synthetic route to pyrrole-based metallo-macrocycles.

X-Ray structural investigations of (2-Ni), (7-Ni), (7-Pd) and (7-Zn-pyr)

The crystal structure determinations of (2-Ni), (7-Ni), (7-Pd) and (7-Zn-pyr) have been carried out.

The structure of (2-Ni) is shown in Fig. 1, and it can be seen that the molecule contains a crystallographic centre of symmetry. The nickel(II) ion (d^8) has a distorted square-planar coordination geometry, with the two independent Ni–S distances equivalent at 2.202(3) and 2.207(4) Å. The benzyl groups are positioned mutually *trans* to each other, minimising steric repulsion.

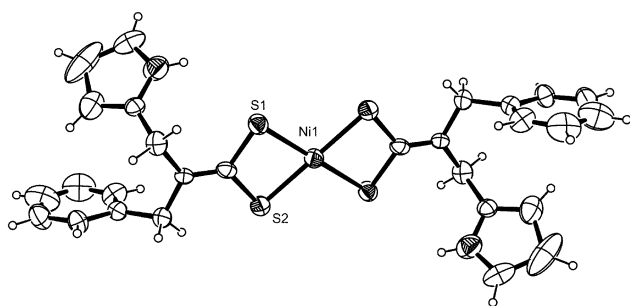


Fig. 1 Crystal structure of (2-Ni) with ellipsoids at 30% probability.

Fig. 2 shows the crystal structure of (7-Ni), which is isomorphous with (7-Pd). Both have their low-spin d^8 metal ions coordinated in a square-planar environment, maximizing LFSE. Illustrative structural parameters for all three metallo-macrocycles are given in Table 1. The pyrrole N–pyrrole N distances tabulated are the lengths of the short and long sides of a parallelogram with a pyrrole N atom at each corner.

The difference in M–S bond length leads to significant changes in the angles subtended at the metal which are 79.0(1)–

Table 1 Selected mean structural parameters for the three crystal structures

	M–M/Å	M–S/Å	pyrrole N–pyrrole N/Å
(7-Ni)	6.63	2.19	3.63, 10.95
(7-Pd)	6.66	2.33	3.65, 11.32
(7-Zn-pyr)	8.54	2.39 ^a	2.96, 11.32

^a Average coordination sphere distance including the Zn–pyr coordinate bond.

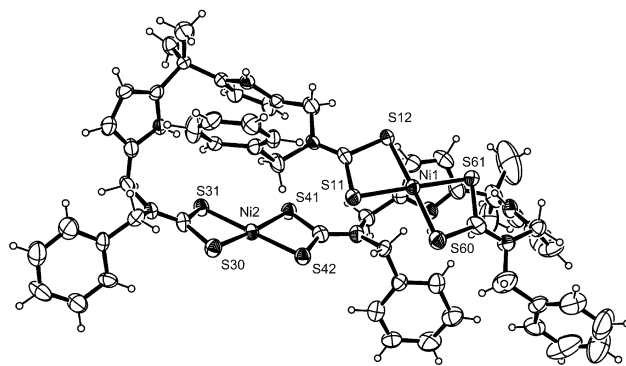


Fig. 2 Crystal structure of (7-Ni) with ellipsoids at 20% probability. The structure of (7-Pd) is isostructural.

80.0(1)° for Ni and 75.2(1)–75.6(1)° for Pd although the overall planarity of the coordination spheres remains unchanged. Least squares planes calculations on the four sulfur atoms in the equatorial planes show that the metal atoms are distorted slightly from the plane (0.07, 0.06 Å for Ni; 0.07, 0.07 Å for Pd) and that in each dimer the two equatorial planes intersect at angles of 32.8 and 33.2°, respectively. The twisted macrocyclic loop adopts a quasi figure-of-eight topology. Binuclear metal

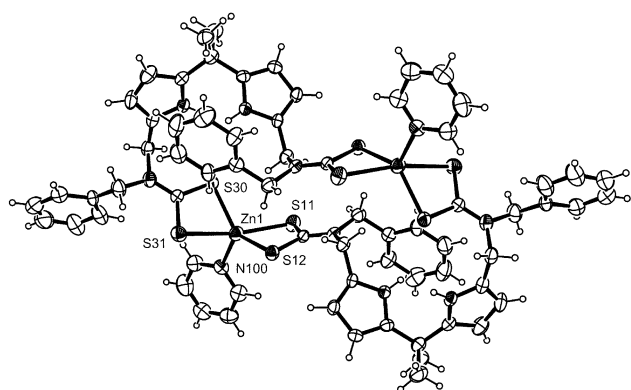


Fig. 3 The structure of (7-Zn-pyr) with thermal ellipsoids at 20% probability.

complexes of cyclooctapyrroles have been shown to adopt a *chiral* figure-of-eight topology.^{30,31}

The structure of the (7-Zn-pyr) complex is shown in Fig. 3, and once again the dimer contains a crystallographic centre of symmetry. Each zinc atom is five-coordinate, so that the coordination sphere of Zn (d^{10}) has a distorted square-based pyramidal geometry with the Zn atom positioned above the basal plane. It is noticeable that the Zn–S bonds to these axial atoms are at 2.555(4), 2.656(4) Å significantly longer than the Zn–S bonds to equatorial atoms S(12) and S(30) which are 2.366(3) and 2.353(3) Å, respectively. Though the structure of (7-Zn-pyr) is complicated by the effects of pyridine coordination to Zn, we see that the macrocyclic loop in this complex remains twisted. In the solid state, the twist in (7-M) has the effect of reducing the size of the cavity within the macrocyclic loop. If this twist is manifested in solution, it may reduce the potency of (7-M) as hosts for anions.

Synthesis of trinuclear cryptands

Analogous Schiff base condensation reactions of 5,5',5''-triformyl-1-ethyltripyrromethane **9**^{32,33} with the appropriate amines followed by NaBH_4 reduction produced the respective amines **12** and **13** (Scheme 3).

Initial attempts to prepare the target metallo-cryptands using an analogous one-pot metallo-dtc procedure produced insoluble products regardless of the identity of the metal salt or the secondary amine reactants suggesting that polymerisation had occurred. However, using less concentrated solutions of reactants, high dilution conditions, the trinuclear metallo-cryptands were isolated in yields ranging from 13 to 87%.

Characterisation

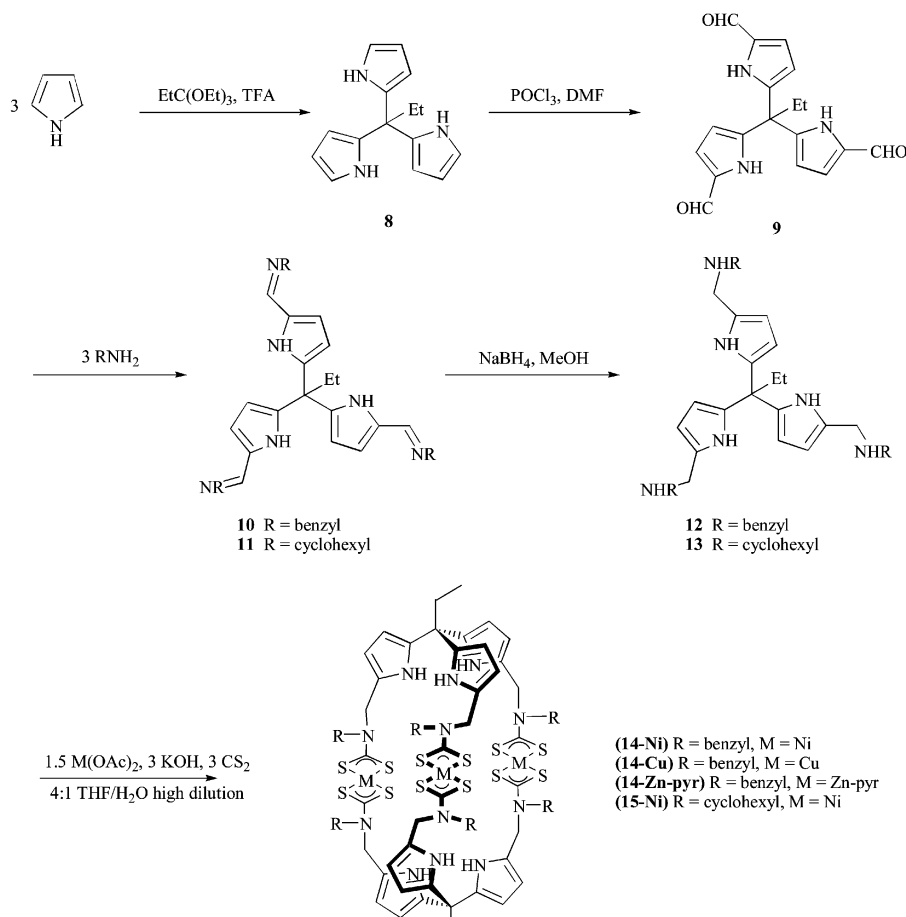
These complexes were characterised by a range of techniques including ^1H NMR, UV-vis spectroscopy, mass spectrometry and elemental analysis (see Experimental section). The neutral metallo-cages are not particularly suitable for ESMS, but they do tend to form adducts with Group 1 metal ions such as Na^+ and K^+ . The addition of a metal salt such as KPF_6 can significantly improve the ESMS spectrum. The ESMS data obtained is tabulated in Table 2 and the spectrum of (15-Ni) is shown in Fig. 4.

Anion binding studies

The use of the pyrrole group in anion recognition has received considerable recent attention. Of particular note are the calixpyrroles, which bind anions *via* the pyrrole NH groups.^{21,22} The anion binding properties of the metallo-macrocycles and -cryptands synthesized here are therefore of interest.

Investigation of the anion binding properties of (7-Ni) and (2-Ni)

The ^1H NMR spectra of the metallo-macrocycles are complex and are not simplified at higher temperature. For this reason,



Scheme 3 Synthetic route to pyrrole-based metallo-cryptands.

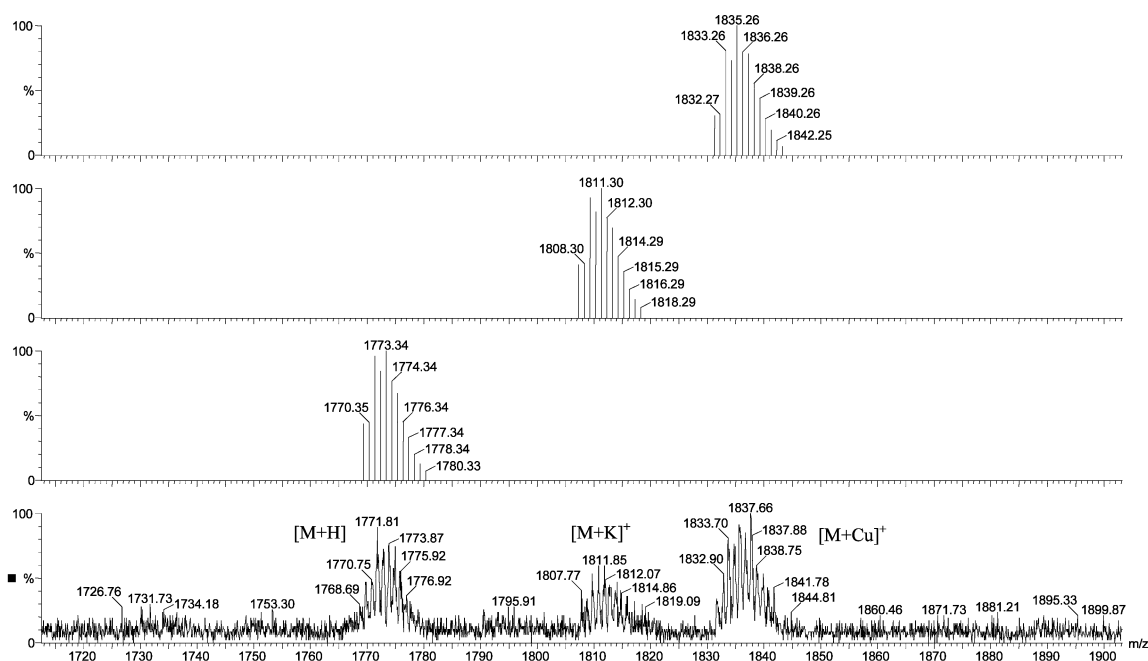


Fig. 4 Observed ESMS spectrum and calculated isotopic clusters for (15-Ni).

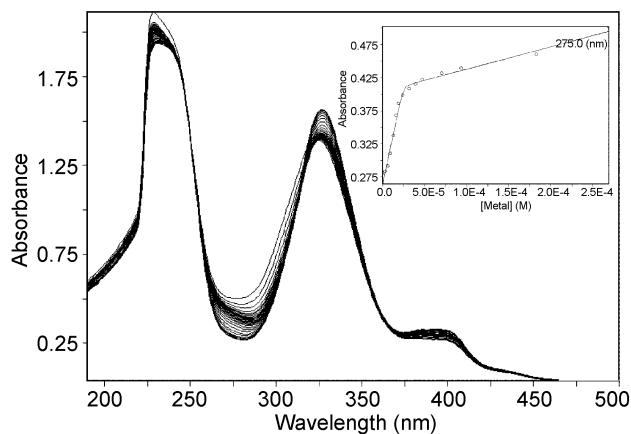


Fig. 5 Changes in the UV-Vis absorption spectrum of (7-Ni) in 70 : 30 DCM-MeCN on the addition of TBA acetate; experimental (circles) and theoretical (line) binding curves for 1 : 1 association (inset).

Table 2 ESMS data for the metallo-cages

Metallo-cage	[M + H] ⁺	[M + Na] ⁺	[M + K] ⁺	[M + Cu] ⁺ ^a
(14-Ni)	—	1843.40	1859.39	—
(15-Ni)	1773.88	—	1810.85	1835.8
(14-Cu)	—	—	1874.46	—

^a Cu⁺ may be present as an impurity in the ESMS spectrometer or acetonitrile solvent.

studies to investigate whether (7-Ni) binds anionic guests were carried out by monitoring changes in the UV-vis spectrum of (7-Ni) in 7 : 3 DCM-MeCN on the addition of aliquots of tetrabutylammonium (TBA) acetate, chloride, bromide and iodide. Substantial shifts (principally in absorbance) in the (7-Ni) spectrum were observed when TBA acetate was added (Fig. 5), allowing the calculation of a stability constant using the Specfit computer program,³⁴ but not for the addition of the other TBA salts. The changes in the UV-Vis spectra of the model compound (2-Ni) and of nickel diethyldithiocarbamate (Ni(dedtc)₂) on the addition of TBA acetate were then recorded under the same conditions to allow comparison (Table 3).

The electronic absorption transition bands were assigned by reference to the literature.^{35,36} Excellent agreement between experiment and binding curves derived theoretically by Specfit³⁴ for 1 : 1 complexation was observed for (7-Ni) and Ni(dedtc)₂, allowing the calculation of the corresponding stability constants; the 1 : 1 stoichiometry was confirmed by Job's method.³⁷ Specfit could not fit the data for (2-Ni), probably due to 2 : 1 acetate : (10-Ni) binding becoming significant at higher acetate concentrations. Interestingly, Ni(dedtc)₂, with no hydrogen bond donor groups, binds acetate with $K \approx 5 \times 10^4 \text{ M}^{-1}$ in the solvent mix used. Although the stability constant for the macrocycle (7-Ni) is significantly larger ($K \approx 1 \times 10^7 \text{ M}^{-1}$), this increased affinity for acetate may be due to the extra Ni atom per molecule, rather than coordination to the pyrrole NHs. This rationalization is in accord with the twisted solid-state structure of the macrocycle: twisting in solution might effectively close the cavity to potential guest species.

Investigation of the anion binding properties of (14-Ni), (15-Ni) and (14-Cu)

Unfortunately, the ¹H NMR spectra of the metallo-cryptands (14-Ni) and (15-Ni) are complex and very broad, and were therefore deemed unsuitable for the study of anion binding. Investigations were however carried out with (14-Cu) by monitoring changes in the UV-vis spectra of CHCl₃ solutions upon addition of aliquots of TBA chloride, benzoate and dihydrogen phosphate. Significant shifts were observed upon addition of TBA benzoate (Fig. 6). The experimental binding curves showed a large change in gradient at a guest concentration of $2.5 \times 10^{-5} \text{ M}$, indicating the formation of a complex of 1 : 1 stoichiometry. Specfit³⁴ was used to calculate a stability constant (Table 4). Surprisingly, the addition of the other TBA salts produced very small shifts, preventing the reliable determination of stability constants with Specfit. This would seem to suggest that (14-Cu) binds benzoate in preference to chloride and dihydrogen phosphate.

Electrochemical study of (14-Cu)

The incorporation of copper(II) centres into the cages introduces a redox active moiety. The potentials at which reduction (Cu^{III}) and oxidation (Cu^{II/III}) occur are dependent upon the environment around the redox centre. Beer's redox active

Table 3 Principal UV-Vis absorptions (200–500 nm), isobestic points and 1 : 1 stability constants with TBA acetate, where applicable, for (7-Ni), (2-Ni) and Ni(dedtc)₂

Complex	LC		MLCT		MLCT		Isobestic point(s)/nm	log ₁₀ K/M ⁻¹ (1:1 complex)
	λ/nm	ε/M ⁻¹ cm ⁻¹	λ/nm	ε/M ⁻¹ cm ⁻¹	λ/nm	ε/M ⁻¹ cm ⁻¹		
(7-Ni)	231	77,600	327	62,500	395	13,200	317	7.06 ± 0.41
(2-Ni)	227, 238 ^a	41,200, 40,800 ^a	328	43,800	395	8,000	297, 254	Not fitted
Ni(dedtc) ₂	240	30,300	325	25,300	388	3,800	293, 253	4.71 ± 0.04

^a Band shoulder.

Table 4 Isobestic point and calculated stability constant for the 1 : 1 (14-Cu)–benzoate complex

Complex	Isobestic point/nm	log ₁₀ K (for 1 : 1 complex)
(14-Cu)	263	5.73 ± 0.18

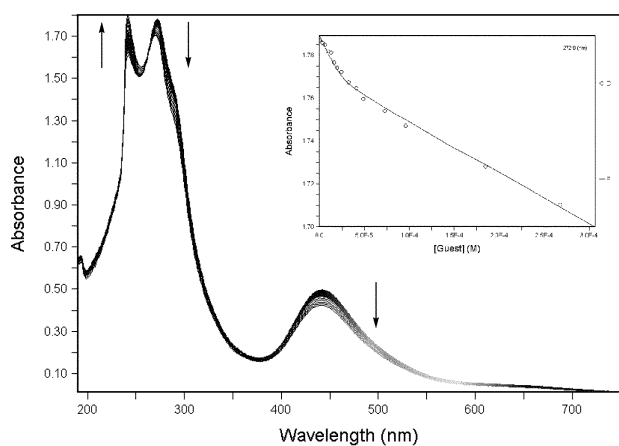


Fig. 6 Changes in the UV-Vis absorption spectrum of (14-Cu) in CHCl₃, upon addition of TBA benzoate; experimental (circles) and theoretical (line) binding curves for 1 : 1 association (inset).

dtc–copper(II) macrocycles demonstrated that the presence of an anionic substrate can affect the redox potential of the Cu^{II/III} dtc redox couple. The resulting cathodic shifts indicate that the presence of the anion stabilises the copper(III) centre.²⁶

The electrochemical studies of (14-Cu) were carried out in DCM using an Ag⁺/Ag reference electrode with TBA tetrafluoroborate as supporting electrolyte. The cyclic voltammograms of (14-Cu) showed both redox couples to be irreversible, with an E_{pa} value of 0.36 V and an E_{pc} of –0.83 V (scan rate 100 mV s⁻¹). The single, broad oxidation and reduction waves, also seen in the square wave voltammograms, suggest three overlapping one-electron waves, implying similar coordination environments for the three copper centers.

Anion binding studies were carried out with 2.5×10^{-6} mol of (14-Cu) in DCM, using an Ag⁺/Ag reference electrode with TBA tetrafluoroborate as supporting electrolyte. The initial square-wave voltammograms (using a scan rate of 100 mV s⁻¹) of both redox couples were recorded, five equivalents of the TBA salt of chloride, benzoate and dihydrogen phosphate were added, and the voltammograms re-recorded.

The square-wave voltammogram for the Cu^{II/III} couple upon the addition of TBA chloride is shown in Fig. 7(a). Upon addition of chloride, the original wave appears to split into two, suggesting that in some way the presence of the halide anion alters both the electronic and stereochemical environments of the copper(II) centres. The splitting into two oxidation peaks was also observed on the addition of benzoate and dihydrogen phosphate, although the effects were not as pronounced. The presence of one cathodically shifted peak is concomitant with anion binding, since the presence of a complexed anion would

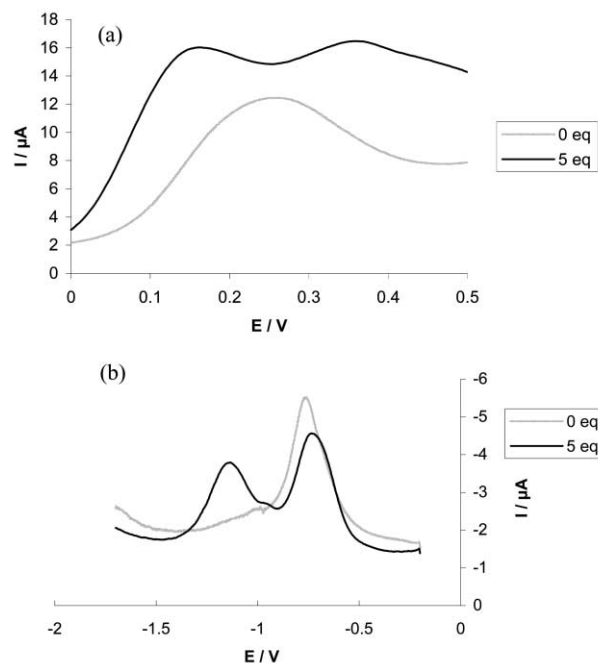


Fig. 7 (a) Changes in the square-wave voltammogram of the Cu^{II/III} couple of (14-Cu) upon the addition of 5 equivalents of TBA chloride. (b) Changes in the square-wave voltammogram of the Cu^{I/II} couple of (14-Cu) upon the addition of 5 equivalents of TBA chloride.

effectively stabilize the copper(III) oxidation state, as seen previously.²⁶

Similar effects were observed in the Cu^{I/II} couple, in that two reduction waves appear on addition of an anionic guest species (Fig. 7(b)). The addition of an anion would once again be expected to produce a cathodic shift in the reduction couple. One wave does indeed appear at a more cathodic potential, while the second wave is only moderately perturbed. This splitting was again observed for all three anions, though the sizes of the two peaks relative to one another altered on changing the anion. For dihydrogen phosphate the peak at the more negative potential dominated, whereas for chloride it was the reverse situation.

The exact cause of this peak splitting is still under investigation. A possible explanation may be that complexation of the anion inside the cryptand results in the copper centers becoming inequivalent. Asymmetric binding of the anion, to only one or two arms of the cryptand, would result in the respective copper centers being in different stereochemical and electronic environments. It is apparent however that the presence of an anion elicits a significant electrochemical response.

Conclusion

The preparation and characterisation of new pyrrole-based dithiocarbamate metallo-macrocycles and cryptands has been described. The bis- and tris-pyrrole compounds have proven to be useful synthons in the metal-directed synthesis of

Table 5 Crystallographic data

	(2-Ni)	(7-Ni)	(7-Pd)	(7-Zn-pyr)
Empirical formula	C ₂₈ H ₂₆ N ₂ NiS ₄	C ₃₈ H ₆₈ N ₈ Ni ₂ O ₄ S ₈	C ₆₀ H ₇₃ N ₈ O _{4.5} Pd ₂ S ₈	C ₇₈ H ₈₀ N ₁₂ S ₈ Zn ₂
Formula weight	577.46	1315.10	1447.54	1572.76
Crystal system	Triclinic	Triclinic	Triclinic	Triclinic
Space group	<i>P</i> $\bar{1}$	<i>P</i> $\bar{1}$	<i>P</i> $\bar{1}$	<i>P</i> $\bar{1}$
<i>a</i> /Å	6.294(10)	12.996(17)	13.160(17)	10.696(15)
<i>b</i> /Å	10.323(14)	16.75(2)	16.82(2)	11.949(15)
<i>c</i> /Å	10.909(17)	17.05(2)	17.26(2)	16.07(2)
<i>a</i> ^o	100.75(1)	68.67(1)	68.39(1)	85.96(1)
<i>β</i> ^o	93.28(1)	83.41(1)	81.78(1)	73.81(1)
<i>γ</i> ^o	106.73(1)	80.28(1)	79.00(1)	79.75(1)
<i>V</i> /Å ³	662.2(17)	3404(7)	3475(8)	1941(5)
<i>Z</i> , <i>D</i> _c /Mg cm ⁻³	1, 1.448	2, 1.283	2, 1.383	1, 1.346
<i>μ</i> /mm ⁻¹	1.068	0.846	1.383	0.884
Unique reflections	2120	11522	11783	6942
Data/restraints/parameters	2120/0/160	11522/0/691	11783/0/733	6942/0/441
Final <i>R</i> indices [<i>I</i> > 2σ(<i>I</i>)], <i>R</i> 1	0.0832	0.0991	0.0762	0.0764
<i>wR</i> 2	0.2298	0.2479	0.2244	0.1185
<i>R</i> indices (all data), <i>R</i> 1	0.1552	0.1638	0.1433	0.1931
<i>wR</i> 2	0.2688	0.2628	0.2632	0.1402
Largest diff. peak, hole/e Å ⁻³	0.490, -0.701	0.626, -0.878	1.111, -1.320	0.415, -0.257

these molecules. X-Ray analysis of the metallo-macrocycles reveals a twisted loop, which effectively reduces the size of the macrocyclic cavity. If present in solution this twisted conformation may account for the apparent lack of anion binding capabilities observed in the UV-vis titration studies. However the nickel macrocycle (7-Ni) was shown to bind acetate. UV-vis anion-binding studies have shown the copper metallo-cryptand (14-Cu) to preferentially bind benzoate. Chloride and dihydrogenphosphate anions produced only small perturbations in the electronic spectrum of the cryptand. Electrochemical studies of the copper cryptand reveal peak splitting of both the oxidation and reduction waves upon addition of anions, although the exact cause of this is still under consideration. It is apparent however that a significant electrochemical response to the presence of anions is observed, and therefore these cryptands warrant further investigation as potential self-assembled anion receptors.

Experimental

General

Elemental analyses were carried out by the Inorganic Chemistry Laboratory Microanalysis Service. NMR spectra were recorded on a Varian Mercury 300 spectrometer, using the deuterated solvent signal as an internal reference. Electro-spray mass spectrometry was carried out on a Micromass LCT spectrometer. UV-Vis spectra were recorded on a Perkin-Elmer Lambda 6 spectrophotometer. Electrochemical studies were carried out on an EG&G Princeton Applied Research Potentiostat/Galvanostat model 273.

Crystal structure determinations

Crystal data for (2-Ni), (7-Ni), (7-Pd) and (7-Zn-pyr) are given in Table 5 together with refinement details. Crystal data was collected with Mo-Kα radiation using the MARresearch Image Plate System. The crystals were positioned at 70 mm from the Image Plate. 100 frames were measured at 2° intervals with a counting time of 2 min. Data analyses were carried out with the XDS program.³⁸ The four structures were solved using direct methods with the Shelx86 program.³⁹ Apart from the solvent molecules, all non-hydrogen atoms were refined with anisotropic thermal parameters. The hydrogen atoms bonded to carbon were included in geometric positions and given thermal parameters equivalent to 1.2 times those of the atom to which they were attached. Empirical absorption corrections were carried out using DIFABS.⁴⁰ The structures were refined on *F*² using Shelx1⁴¹ to convergence.

CCDC reference numbers 195408–195411

See <http://www.rsc.org/suppdata/dt/b2/b210099a/> for crystallographic data in CIF or other electronic format.

General procedure for preparation of the dtc complexes (2-M)

1*H*-pyrrol-2-ylmethylbenzylamine **1** (1 equivalent, prepared as previously reported)⁴² was dissolved in THF and CS₂ (1.1 equivalents) added. KOH (1 equivalent) and the M(II) salt (1 equivalent, see below) were dissolved in water and added to the solution, the base was added before the M(II) salt. The THF : H₂O ratio (by volume) after addition of both the base and the M(II) salt was 4 : 1. The mixture was allowed to stir at room temperature for 10 h and at this point, more water was added until a solid precipitate was obtained. This was filtered off and recrystallised from DCM–EtOH: for (2-Ni), the solid recovered included crystals suitable for analysis by single crystal X-ray diffraction.

(2-Ni). Colour: dark green; M(II) salt = Ni(OAc)₂·4H₂O; yield = 50%; ¹H NMR (CDCl₃): δ 4.92 (s, 4H, CH₂Ph), 5.06 (s, 4H, CH₂-pyrrole), 6.15 (s, 4H, pyrrole H3 + H3' overlapping pyrrole H4 + H4'), 6.84 (s, 2H, pyrrole H5 + H5'), 7.40 (br m, 10H, Ph), 9.14 (br s, 2H, pyrrole NH). Analysis: Calc. for C₂₆H₂₆N₄S₄Ni: C, 53.7, H, 4.5, N, 9.6. Found: C, 53.7, H, 4.5, N, 9.5%; ESMS [C₂₆H₂₆N₄S₄Ni + Cl]⁻: *m/z* observed 615.08, calc. 615.01.

(2-Zn). Colour: white; M(II) salt = Zn(OAc)₂·4H₂O; yield = 42%; ¹H NMR (CDCl₃): δ 4.60 (s, 4H, CH₂Ph), 4.71 (s, 4H, CH₂-pyrrole), 6.14 (s, 4H, pyrrole H3 + H3' overlapping pyrrole H4 + H4'), 6.83 (s, 2H, pyrrole H5 + H5'), 7.35 (br m, 10H, Ph), 8.79 (br s, 2H, pyrrole NH). Analysis: Calc. for C₂₆H₂₆N₄S₄Zn·3H₂O: C, 48.6, H, 5.0, N, 8.7. Found: C, 48.5, H, 4.1, N, 8.4%; ESMS [C₂₆H₂₆N₄S₄Zn - H]⁻: *m/z* observed 585.37, calc. 585.02.

5, 5'-Diformyl-1,1-dimethyldipyrromethane 4

1,1-Dimethyldipyrromethane **3** (5.69 g, 32.7 mmol, prepared as previously reported)⁵ was dissolved in DMF (50 ml) and benzoyl chloride (21 ml) added slowly at 0 °C. The solution was stirred at this temperature for 2 h and then at room temperature for a further 2 h, at which point the imine salt began to precipitate. To ensure complete precipitation, toluene (50 ml) was added and the mixture stirred for a further hour. The imine salt was filtered off and dissolved immediately in 70% aqueous ethanol (100 ml) containing Na₂CO₃ (5.0 g). This mixture was refluxed for 15 min, diluted

with water (125 ml) and the resulting precipitate collected and recrystallised from EtOH to give 5.09 g (22.1 mmol, 68%) of **4** as a pale yellow solid: $^1\text{H NMR}$ (CDCl_3): δ 1.76 (3, 6H, CH_3), 6.24 (m, 2H, pyrrole H3 + H3'), 6.85 (m, 2H, pyrrole H4 + H4'), 9.27 (s, 2H, CHO), 10.89 (br s, 2H, pyrrole NH).

Imine 5

Imine **5** was prepared by a modification of a previously reported method.⁹ 5.09 g (22.1 mmol) of 5, 5'-diformyl-1,1-dimethylpyrromethane **4** was dissolved in THF (70 ml) and cooled to 0 °C. Benzylamine (5.2 ml) was added dropwise. After 15 min, the solution was allowed to warm to room temperature and stirred for 10 h. The solvent was removed under reduced pressure and the resulting solid recrystallised from the minimum volume of hot Et₂O to give 8.08 g (19.8 mmol, 89%) of imine **5** as a pale yellow solid: $^1\text{H NMR}$ (CDCl_3): δ 1.66 (s, 6H, CH_3), 4.66 (s, 4H, CH_2Ph), 6.07 (d, 2H, J 3.5 Hz, pyrrole H3 + H3'), 6.42 (d, 2H, J 3.5 Hz, pyrrole H4 + H4'), 7.30 (m, 10H, Ph), 8.04 (s, 2H, $\text{CH}=\text{N}-$); ESMS [$\text{C}_{27}\text{H}_{28}\text{N}_4 + \text{H}$]⁺: m/z observed 409.24, calc. 409.30.

Amine 6

Amine **6** was prepared by a modification of a previously reported method.⁹ Imine **5** (1.0 g, 2.45 mmol) was dissolved in deoxygenated methanol (100 ml) and NaBH_4 (0.5 g) added slowly at 0 °C. The solution was allowed to warm to room temperature and then refluxed for 10 h. The solvent was partially evaporated and 50 ml of water added to destroy the excess NaBH_4 . The water layer was extracted three times with 30 ml of Et₂O, and the Et₂O fractions combined and dried over MgSO_4 . Filtration and evaporation of the solvent gave 0.57 g (1.38 mmol, 56%) of amine **6** as a white fluffy solid: $^1\text{H NMR}$ (CDCl_3): δ 1.62 (s, 6H, CH_3), 3.63 (s, 4H, CH_2Ph), 3.65 (s, 4H, CH_2 -pyrrole) 5.92 (m, 4H, pyrrole H3 + H3' overlapping pyrrole H4 + H4'), 7.25 (m, 10H, Ph), 8.47 (br s, 2H, CH_2NHCH_2). Analysis: Calc. for $\text{C}_{27}\text{H}_{32}\text{N}_4$: C, 78.6, H, 7.8, N, 13.6. Found: C, 78.3, H, 8.0, N, 13.4%; ESMS [$\text{C}_{27}\text{H}_{32}\text{N}_4 + \text{H}$]⁺: m/z observed 413.22, calc. 413.27.

General procedure for preparation of the dtc macrocycles (7-M)

Amine **6** (1 equivalent) was dissolved in THF and CS_2 (2.2 equivalents) added. KOH (2 equivalents) and the M(II) salt (1 equivalent, see below) were dissolved in water and added to the solution; the base was added before the M(II) salt. The THF: H_2O ratio (by volume) after addition of both the base and the M(II) salt was 4 : 1. The mixture was allowed to stir at room temperature for 10 h; at this point, more water was added until a solid precipitate was obtained. This was filtered off and purified as described below.

(7-Ni). Colour: dark green; M(II) salt = $\text{Ni}(\text{OAc})_2 \cdot 4\text{H}_2\text{O}$; chromatographed on silica (CHCl_3) with the forerunning band collected and recrystallised from 1,2-dichloroethane-diisopropyl ether giving X-ray quality crystals; yield = 86%; $^1\text{H NMR}$ (CDCl_3): δ 1.65 (s, 6H, CH_3), 4.45–5.00 (br m, 16H, CH_2Ph overlapping CH_2 -pyrrole), 5.80–6.36 (br m, 8H, pyrrole H3 + H3' overlapping pyrrole H4 + H4'), 7.00–7.50 (br m, 20H, Ph), 8.08–8.50 (br m, 4H, pyrrole NH). Analysis: Calc. C, 52.3, H, 5.3, N, 8.4 for $\text{C}_{58}\text{H}_{60}\text{N}_8\text{S}_8\text{Ni}_2 \cdot 5\text{H}_2\text{O}$. Found: C, 52.0, H, 5.3, N, 7.8%.

(7-Pd). Colour: yellow; M(II) salt = K_2PdCl_4 ; chromatographed on silica (CHCl_3) with the forerunning band collected and recrystallised from 1,2-dichloroethane-diisopropyl ether giving X-ray quality crystals; yield = 68%; $^1\text{H NMR}$ (CDCl_3): δ 1.60 (s, 6H, CH_3), 4.65–4.93 (br m, 16H, CH_2Ph overlapping CH_2 -pyrrole), 5.87–6.28 (br m, 8H, pyrrole H3 + H3'

overlapping pyrrole H4 + H4'), 7.10–7.43 (br m, 20H, Ph), 8.01–8.37 (br m, 4H, pyrrole NH). Analysis: Calc. C, 49.4, H, 4.9, N, 7.9 for $\text{C}_{58}\text{H}_{60}\text{N}_8\text{S}_8\text{Pd}_2 \cdot 4\text{H}_2\text{O}$. Found: C, 49.0, H, 4.8, N, 7.3%; ESMS [$\text{C}_{58}\text{H}_{60}\text{N}_8\text{S}_8\text{Pd}_2 + \text{K}$]⁺: m/z observed 1377.08, calc. 1377.04.

(7-Zn-pyr). Colour: white; M(II) salt = $\text{Zn}(\text{OAc})_2 \cdot 2\text{H}_2\text{O}$; dissolved in pyridine and precipitated by addition of water; recrystallised from pyridine-di-*n*-butyl ether giving X-ray quality crystals; yield = 87%; $^1\text{H NMR}$ (CDCl_3): δ 1.57 (s, 12H, CH_3), 4.86 (s, 8H, CH_2Ph), 5.20 (s, 8H, pyrrole- CH_2), 5.90 (s, 4H, pyrrole H3 + H3'), 6.08 (s, 4H, pyrrole H4 + H4'), 7.14–7.24 (m, 26H, Ph overlapping pyridine H3 + H4 + H5), 7.86 (m, 4H, pyrrole NH), 8.84 (m, 4H, pyridine H2 + H6). Analysis: Calc. for $\text{C}_{68}\text{H}_{70}\text{N}_{10}\text{S}_8\text{Zn}_2$: C, 57.7, H, 5.0, N, 9.9. Found: C, 57.4, H, 4.9, N, 9.9%.

1-Ethyltripyrromethane 8

1-Ethyltripyrromethane **8** was prepared by the method of Lindsey and coworkers³² as modified by Wang and Bruce.³³ Triethyl orthopropionate (8.2 ml) was dissolved in an excess of freshly distilled pyrrole (50 ml). TFA (0.5 ml) was added and the mixture stirred under nitrogen; the solution turned dark red in colour. After 5 min, the reaction was quenched with 0.2 M NaOH (50 ml) giving a bright yellow emulsion. Ethyl acetate (50 ml) was added and the organic phase separated and dried over anhydrous MgSO_4 . Ethyl acetate and unreacted pyrrole were removed under reduced pressure to yield the crude product, which was stirred in cold ethanol. The product was filtered off, washed with cold ethanol and dried under vacuum to give 5.59 g (23.4 mmol, 57%) of **8** as a white powder; $^1\text{H NMR}$ (CDCl_3): δ 0.92 (t, 3H, J 7.3 Hz, CH_3), 2.32 (q, 2H, J 7.3 Hz, CH_2CH_2), 6.18 (m, 6H, pyrrole H3 + H3' + H3'' overlapping pyrrole H4 + H4' + H4''), 6.65 (q, 3H, H5 + 5' + 5''), d 7.89 (br s, 3H, NH).

5,5',5''-Triformyl-1-ethyltripyrromethane 9

5,5',5''-Triformyl-1-ethyltripyrromethane **9** was prepared using a modification of previously reported methods.⁴³ 1-Ethyltripyrromethane **8** (3.0 g, 12.6 mmol) was dissolved in dry DMF (115 ml) and cooled to 0 °C. POCl_3 (7.0 ml) was added dropwise. The mixture was heated to 60 °C for 2 h and then hydrolysed (80 °C) in water (1.3 l) containing NaOH (19.2 g). The product precipitated out as a brown solid after 1 h and was filtered off, dried under vacuum and purified by column chromatography on silica (DCM–MeOH, 50:1 v/v) to give 2.768 g of **9** (8.57 mmol, 68%) as a fluffy white solid; $^1\text{H NMR}$ (CDCl_3): d 1.00 (t, 3H, J 6.8 Hz, CH_3), d 2.60 (q, 2H, J 6.8 Hz, CH_2CH_2), 6.22 (s, 3H, pyrrole H3 + H3' + H3''), 6.88 (s, 3H, pyrrole H4 + H4' + H4''), 9.08 (s, 3H, CHO), 11.53 (s, 3H, pyrrole NH).

Imine 10

Imine **10** was prepared by a modification of a previously reported method.⁴² 5,5',5''-Triformyl-1-ethyltripyrromethane **9** (750 mg, 2.32 mmol) was dissolved in THF (85 ml) and cooled to 0 °C. Benzylamine (3.3 equivalents) was added dropwise. After 15 min, the solution was stirred at 60 °C for 15 h. The solvent was removed under reduced pressure and the resultant solid recrystallised from DCM–hexane to give 1.15 g (1.95 mmol, 84%) of imine **10** as dark red crystals: $^1\text{H NMR}$ (CDCl_3): δ 0.89 (t, 3H, J 7.2 Hz, CH_3), 2.41 (q, 2H, J 7.2 Hz, CH_2CH_2), 4.64 (s, 6H, CH_2Ph), 6.12 (d, 3H, J 3.5 Hz, pyrrole H3 + H3' + H3''), 6.42 (d, 3H, J 3.5 Hz, pyrrole H4 + H4' + H4''), 7.30 (br m, 15H, Ph), 8.04 (s, 3H, $\text{CH}=\text{N}-$).

Imine 11

Imine **11** was prepared similarly to imine **10**. 5,5',5''-Triformyl-1-ethyltripyrromethane **9** (1.02 g, 3.16 mmol) was dissolved in

THF (40 ml) and cooled to 0 °C. Cyclohexylamine (3.3 equivalents) was added dropwise. After 15 min the mixture was stirred at 60 °C for 15 h. The solvent was removed under reduced pressure and the resultant oil was placed under vacuum to remove any unreacted amine and residual solvent, giving 1.55 g (2.98 mmol, 94%) of imine **11** as a light pink fluffy solid; ¹H NMR (CDCl₃): δ 0.95 (t, 3H, CH₃), 1.00–1.90 (m, 30H, cyclohexyl-CH₂), 2.55 (q, 2H, CH₃CH₂), 3.10 (m, 3H, cyclohexyl-CH), 6.10 (s, 3H, H3 + 3' + 3''), 6.42 (s, 3H, H4 + 4' + 4''), 7.90 (s, 3H, CH=N-).

Amine 12

Amine **12** was prepared by a modification of a previously reported method.⁴² Imine **10** (1.15 g, 1.95 mmol) was dissolved in deoxygenated methanol (150 ml) and excess NaBH₄ (4.50 g) added slowly at 0 °C. The solution was allowed to warm to room temperature and then refluxed under nitrogen for 2 h. Solvent was partially evaporated and 100 ml water added to destroy the excess NaBH₄. The water layer was extracted 3 times with 60 ml of Et₂O, and the Et₂O fractions combined and dried over MgSO₄. Filtration and removal of the solvent under reduced pressure gave 706 mg (1.18 mmol, 61%) of amine **12** as a yellow oil, which was used without further purification; ¹H NMR (CDCl₃): δ 0.91 (t, 3H, J 7.3 Hz, CH₃), 2.30 (q, 2H, J 7.3 Hz, CH₃CH₂), 3.67 (s, 6H, CH₂Ph), 3.68 (s, 6H, CH₂-pyrrole), 5.96 (m, 3H, pyrrole H3 + H3' + H3''), 6.01 (m, 3H, pyrrole H4 + H4' + H4''), 7.25 (m, 15H, Ph), 8.27 (br s, 3H, CH₂NHCH₂).

Amine 13

Amine **13** was prepared similarly to amine **12**. Imine **11** (1.46 g, 2.80 mmol) was reacted to give 1.28 g (2.49 mmol, 89%) of amine **13** as a yellow oil, which was used without further purification; ¹H NMR (CDCl₃): δ 0.90 (t, 3H, J Hz, CH₃), 1.00–2.00 (m, 30H, cyclohexyl-CH₂), 2.30 (q, 2H, J Hz, CH₃CH₂), 2.39 (m, 3H, cyclohexyl-CH), 3.65 (s, 6H, NHCH₂-pyrrole), 5.91 (s, 6H, pyrrole H3 + H3' + H3'') overlapped with H4 + H4' + H4''), 8.72 (br s, 3H, CH₂NH-cyclohexyl).

General procedure for preparation of the dtc cages (14-M) and (15-M)

The amine **12** or **13** was dissolved in THF (to give a concentration of approximately 1 × 10⁻³ M) and CS₂ (3.3 equivalents) added. KOH (3 equivalents) and the M(II) acetate salt (1.5 equivalents) were dissolved in water and added to the solution; the base was added before the M(II) salt. The THF : H₂O ratio (by volume) after addition of both the base and M(II) salt was 4 : 1. The mixture was allowed to stir at room temperature for 15 h; at this point, THF was evaporated under reduced pressure and more water added to give a solid precipitate, except in the case of (**15-Ni**). This was purified as stated below.

(**14-Ni**). The lime green solid was purified by column chromatography on silica (100 : 1 CHCl₃-MeOH) with the forerunning band collected and recrystallised from DCM-EtOH; yield = 87%; ¹H NMR (CDCl₃): δ 0.89–1.10 (br s, 6H, CH₃), 2.10–2.40 (br s, 4H, CH₃CH₂), 4.40–4.90 (br m, 24 H, CH₂-pyrrole overlapped with CH₂Ph), 5.90–6.40 (br m, 12H, pyrrole H3 + H3' + H3'') overlapped with pyrrole H4 + H4' + H4''), 7.00–7.40 (br m, 30H, PhH), 8.20–8.60 (br m, 6H, pyrrole NH); ESMS [C₈₄H₈₂N₁₂S₁₂Ni₃ + K]⁺: *m/z* observed 1859.39, calc. 1859.11. Analysis: Calc. for C₈₂H₈₈N₁₂S₁₂Ni₃·4H₂O: C, 52.5, H 5.2, N, 9.0. Found: C, 52.4, H, 4.2, N, 9.0%

(**14-Zn-pyr**). The pink solid was dissolved in minimum pyridine and precipitated by adding water, filtered and washed with EtOH and Et₂O to give a pale pink solid; yield = 13%. Analysis:

Calc. for C₉₉H₉₇N₁₅S₁₂Zn₃: C, 57.2, H, 4.7, N, 10.1. Found: C, 56.7, H, 4.7, N, 9.8%

(**14-Cu**). The dark brown solid was recrystallised from DCM-EtOH to give the pure product; yield = 67%; ESMS [C₈₄H₈₂N₁₂S₁₂Cu₃ + K]⁺, *m/z* observed 1874.46, calc. 1874.09. Analysis: Calc. for C₈₄H₈₂N₁₂S₁₂Cu₃·5H₂O: C, 52.4, H, 4.8, N, 8.7. Found: C, 52.2, H, 4.5, N, 8.8%

(**15-Ni**). The green solid was chromatographed on silica (DCM-MeOH, 100 : 1) with the forerunning band collected and recrystallised from DCM-EtOH; yield = 51%; ¹H NMR (CDCl₃): δ 0.80–2.10 (br m, 66H, CH₃ overlapped with cyclohexyl-CH₂), 2.30–2.50 (br s, 10H, CH₃CH₂ overlapped with cyclohexyl-CH), 4.20–4.40 (br s, 12H, CH₂-pyrrole), 5.90–6.40 (br m, 12H, pyrrole H3 + H3' + H3'') overlapped with pyrrole H4 + H4' + H4''), 8.20–9.20 (br m, 6H, pyrrole NH); ESMS [C₇₈H₁₀₀N₁₂S₁₂Ni₃ + H]⁺, *m/z* observed 1773.88, calc. 1773.33. Analysis: Calc. for C₇₈H₁₀₆N₁₂S₁₂Ni₃: C, 52.9, H, 6.0, N, 9.5. Found: C, 52.7, H, 5.7, N, 9.4%

Acknowledgements

We thank the EPSRC for a postdoctoral fellowship (O. D. F., E. J. H.) and the EPSRC and the University of Reading for funds for the Image Plate system (M. G. B. D.).

References

- 1 R. W. Saalfrank and I. Bernt, *Curr. Opin. Solid State Mater. Sc.*, 1998, **3**, 407.
- 2 M. Fujita, *Chem. Soc. Rev.*, 1998, **27**, 417.
- 3 B. Leininger, B. Olenyuk and P. J. Stang, *Chem. Rev.*, 2000, **100**, 853.
- 4 C. J. Jones, *Chem. Soc. Rev.*, 1998, **27**, 289.
- 5 B. Linton and A. D. Hamilton, *Chem. Rev.*, 1997, **97**, 1669.
- 6 A. W. Maverick, S. C. Buckingham, Q. Yao, J. R. Bradbury and G. S. Stanley, *J. Am. Chem. Soc.*, 1986, **108**, 7430.
- 7 D. A. McMorran and P. J. Steel, *Angew. Chem., Int. Ed.*, 1998, **37**, 3295.
- 8 D. L. Caulder and K. N. Raymond, *J. Chem. Soc., Dalton Trans.*, 1999, 1185.
- 9 R. W. Saalfrank, I. Bernt, E. Uller and F. Hampel, *Angew. Chem., Int. Ed. Engl.*, 1997, **36**, 2482.
- 10 M. Fujita, S. Hagao and K. Ogura, *J. Am. Chem. Soc.*, 1995, **117**, 1649.
- 11 M. Aoyagi, K. Biradha and M. Fujita, *J. Am. Chem. Soc.*, 1999, **121**, 7457.
- 12 B. Hasenkopf, J.-M. Lehn, N. Boumediene, A. Dupont-Gervais, A. V. Dorsselaer, B. Kneisel and D. Fenske, *J. Am. Chem. Soc.*, 1997, **119**, 10956.
- 13 P. J. Stang and B. Olenyuk, *Acc. Chem. Res.*, 1997, **30**, 502.
- 14 R. M. Nielson, J. T. Hupp and E. I. Yoon, *J. Am. Chem. Soc.*, 1995, **117**, 9085.
- 15 M. Albrecht, *Chem. Rev.*, 2001, **101**, 3457.
- 16 M. Albrecht, *Chem. Soc. Rev.*, 1998, **27**, 281.
- 17 J. Setsune, T. Yokoyama, S. Muraoka, H. Huang and T. Sakurai, *Angew. Chem., Int. Ed.*, 2000, **39**, 1115.
- 18 A. Thompson and D. Dolphin, *J. Org. Chem.*, 2000, **65**, 7870.
- 19 A. Thompson, S. J. Rettig and D. Dolphin, *Chem. Commun.*, 1999, 631.
- 20 Y. Zhang, A. Thompson, S. J. Rettig and D. Dolphin, *J. Am. Chem. Soc.*, 1998, **120**, 13537.
- 21 P. A. Gale, P. J. Anzenbacher and J. L. Sessler, *Coord. Chem. Rev.*, 2001, **222**, 57.
- 22 P. A. Gale, J. L. Sessler and V. Kral, *Chem. Commun.*, 1998, **1**, 1.
- 23 O. D. Fox, T. D. Rolls, M. G. B. Drew and P. D. Beer, *Chem. Commun.*, 2001, 1632.
- 24 O. D. Fox, E. J. S. Wilkinson, P. D. Beer and M. G. B. Drew, *Chem. Commun.*, 2000, **5**, 391.
- 25 O. D. Fox, M. G. B. Drew and P. D. Beer, *Angew. Chem., Int. Ed.*, 2000, **39**, 136.
- 26 P. D. Beer, N. Berry, M. G. B. Drew, O. D. Fox, M. E. Padilla-Tosta and S. Patel, *Chem. Commun.*, 2001, 199.
- 27 L. H. Uppadine, J. M. Weeks and P. D. Beer, *J. Chem. Soc., Dalton Trans.*, 2001, **22**, 3367.
- 28 N. Berry, M. D. Pratt, O. D. Fox and P. D. Beer, *Supramol. Chem.*, 2001, **13**, 677.

-
- 29 M. E. Padilla-Tosta, O. D. Fox, M. G. B. Drew and P. D. Beer, *Angew. Chem., Int. Ed.*, 2001, **40**, 4235.
- 30 A. Werner, M. Michels, L. Zander, J. Lex and E. Vogel, *Angew. Chem., Int. Ed.*, 1999, **38**, 3650.
- 31 T. D. Lash, *Angew. Chem., Int. Ed.*, 2000, **39**, 1763.
- 32 B. J. Littler, M. A. Miller, C.-H. Hung, R. W. Wagner, D. F. O'Shea, P. D. Boyle and J. S. Lindsey, *J. Org. Chem.*, 1999, **64**, 1391.
- 33 Q. M. Wang and D. W. Bruce, *Synlett*, 1995, 1267.
- 34 R. A. Binstead, B. Jung and A. D. Zuberbuhler, Specfit/32 Global Analysis System, Spectrum Software Associates, Chapel Hill, NC, 2000.
- 35 D. Oktavec, B. Siles, J. Stefanec, E. Korgova and J. Garaj, *Collect. Czech. Chem. Commun.*, 1980, **45**, 791.
- 36 K. B. Pandeya, T. S. Waraich, R. C. Gaur and R. P. Singh, *J. Inorg. Nucl. Chem.*, 1981, **43**, 3159.
- 37 V. M. S. Gil and N. C. Oliveira, *J. Chem. Educ.*, 1990, **67**, 473.
- 38 W. Kabsch, *J. Appl. Crystallogr.*, 1988, **21**, 916.
- 39 Shelx86: G. M. Sheldrick, *Acta Crystallogr., Sect. A*, 1990, **46**, 467.
- 40 DIFABS: N. Walker and D. Stuart, *Acta Crystallogr., Sect. A*, 1983, **39**, 158.
- 41 G. M. Sheldrick, Shelxl: program for crystal structure refinement. 1993, University of Gottingen.
- 42 B. de Bruin, R. J. N. A. M. Kicken, N. F. A. Suos, M. P. J. Donners, C. J. den Reijer, A. J. Sandee, R. de Gelder, J. M. M. Smits, A. W. Gal and A. L. Spek, *Eur. J. Inorg. Chem.*, 1999, 1581.
- 43 J. A. de Groot, R. van der Steen, R. Fokkens and J. Lugtenburg, *Recueil*, 1982, **101**, 35.